

Mass Spectrometry Uncovers Molecular Reactivities of Coordination and Organometallic Gold(III) Drug Candidates in Competitive Experiments That Correlate with Their Biological Effects

Samuel M. Meier,^{*,†} Christopher Gerner,[†] Bernhard K. Keppler,^{‡,§} Maria Agostina Cinelli,^{||} and Angela Casini^{*,⊥}

[†]Department of Analytical Chemistry, University of Vienna, Waehringer Str. 38, 1090 Vienna, Austria

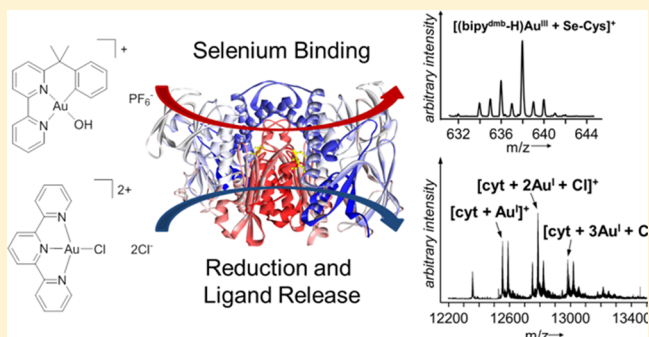
[‡]Institute of Inorganic Chemistry, [§]Research Platform "Translational Cancer Therapy Research", University of Vienna, Waehringer Str. 42, 1090 Vienna, Austria

^{||}University of Sassari, Dipartimento di Chimica e Farmacia, Via Vienna 2, Sassari I-07100, Italy

[⊥]School of Chemistry, Cardiff University, Main Building, Park Place, CF10 3AT Cardiff, United Kingdom

Supporting Information

ABSTRACT: The reactivity of three cytotoxic organometallic gold(III) complexes with cyclometalated C,N,N and C,N ligands (either six- or five-membered metallacycles), as well as that of two representative gold(III) complexes with N-donor ligands, with biological nucleophiles has been studied by ESI-MS on ion trap and time-of-flight instruments. Specifically, the gold compounds were reacted with mixtures of nucleophiles containing L-histidine (imine), L-methionine (thioether), L-cysteine (thiol), L-glutamic acid (carboxylic acid), methyl-seleno-L-cysteine (selenoether), and *in situ* generated seleno-L-cysteine (selenol) to judge the preference of the gold compounds for binding to selenium-containing amino acid residues. Moreover, the gold compounds' reactivity was studied with proteins and nucleic acid building blocks. These experiments revealed profound differences between the coordination and organometallic families and even within the family of organometallics, which allowed insights to be gained into the compounds mechanisms of action. In particular, interactions with seleno-L-cysteine appear to reflect well the compounds' inhibition properties of the seleno-enzyme thioredoxin reductase and to a certain extent their antiproliferative effects *in vitro*. Therefore, mass spectrometry is successfully applied for linking the molecular reactivity and target preferences of metal-based drug candidates to their biological effects. Finally, this experimental setup is applicable to any other metallodrug that undergoes ligand substitution reactions and/or redox changes as part of its mechanism of action.



INTRODUCTION

In modern medicinal inorganic chemistry, a large number of different metal complexes with considerable antiproliferative properties against different cancer types were identified *in vitro* and *in vivo*, often showing improved effects and innovative modes of action with respect to those of classical platinum anticancer agents.^{1–5} In particular, gold compounds have received considerable attention in recent years, among which are those stabilized by phosphines, nitrogen-containing or alkynyl ligands, dithiocarbamates, or even as gold nanoparticles.^{6–10} Furthermore, auranofin, a gold(I) drug to treat rheumatoid arthritis, has been repurposed and is in clinical studies against chronic lymphatic leukemia¹¹ as well as for the treatment of ovarian cancer.¹²

In spite of their promising anticancer effects, the risk in developing gold(III) coordination compounds for biological applications is that they may be characterized by a remarkable

oxidizing character of the metal center under physiological conditions. While redox activity may be an advantage to induce the desired anticancer effects, uncontrolled redox reactions in biological environments may lead to side effects and to the compound's inactivation. In general, both organometallic gold(I) and gold(III) compounds have increased stability with respect to classical gold-based coordination complexes and are very suitable for designing gold compounds that still act as pro-drugs but in which the redox properties and ligand exchange reactions can be modulated, e.g., to achieve selective activation in diseased cells.¹³ The families of bioactive gold organometallics developed so far include cyclometalated gold(III) complexes, gold(I) and gold(III) NHC–carbene complexes, and gold(I) alkynyl complexes.^{13–15} Interestingly,

Received: January 1, 2016

cyclometalated complexes are generally characterized by redox and thermodynamic stability, and their steric and electronic properties can be tuned by modification of either the anionic cyclometalated or the ancillary ligands, e.g., to achieve compounds with optimized lipophilic character. Thus, a variety of gold(III) complexes of this family have been synthesized as possible anticancer agents, featuring both bidentate C,N-donor and terdentate C,N,N-, C,N,C-, and N,C,N-donor ligands with either five- or six-membered C,N metallacycles.^{13,16}

Overall, for all of these classes of gold coordination and organometallic compounds, interactions with proteins, i.e., enzymes, are considered to be the determining factor for their observed biological and anticancer effects, whereas interactions with nucleic acids appear to be markedly less relevant, with a few exceptions.^{7,17} In this respect, gold compounds constitute a valid alternative to platinum-based chemotherapies. The reaction mechanism of different gold(III) coordination compounds bearing N-donor ligands (e.g., bipyridine, terpyridine, etc.) with amino acids and peptides and the structural characterization of the resulting gold adducts have been investigated via different methods, including various spectroscopies, X-ray crystallography, and mass spectrometry techniques.¹⁷ In addition, the reactivity of gold(III) compounds/ions with model amino acids and peptides has also been explored, in some cases allowing structural characterization of the resulting adducts.¹⁸

Fewer studies are available concerning cyclometalated gold(III) compounds and their reactivity with biomolecules, which highlights the differences and possible advantages in developing organometallic compounds with respect to classical coordination complexes. Among the few reported studies, cytotoxic cationic dinuclear oxo-bridged complexes $[(C,N,N)_2Au_2(\mu-O)](PF_6)_2$ (with CH,N,N = 6-(1,1-dimethylbenzyl)-2,2'-bipyridine or 6-(1-methylbenzyl)-2,2'-bipyridine) and their corresponding mononuclear hydroxido complexes were evaluated for their reactivity with model proteins by mass spectrometry.¹⁹ The obtained results evidenced that the resulting gold–protein adducts still contain gold ions in the +3 oxidation state and that the multidentate ligands are retained, at variance with what has been previously reported for other dinuclear and mononuclear gold(III) compounds bearing exclusively N-donor ligands.²⁰

Notably, among the recognized targets for gold compounds, the seleno-enzyme thioredoxin reductase (TrxR) has been widely investigated.²¹ Interestingly, human TrxR contains a cysteine-selenocysteine redox pair at the C-terminal active site, and the solvent-accessible selenolate group, arising from enzymatic reduction, constitutes a likely target for “soft” metal ions such as gold. The direct binding of gold(I)/(III) compounds to the tetrapeptide Ac-Gly-[Cys-Sec]-Gly-NH₂, reproducing the C-terminal motif of TrxR, has been demonstrated by mass spectrometry,^{22,23} whereas additional evidence of the binding of gold(I) complexes to the selenol moiety of purified TrxR was obtained via biochemical assays.^{19,24} Interestingly, cyclometalated gold(III) coordination compounds showed less selectivity for binding to selenol groups relative to that for thiols in TrxR, and oxidation of thiol/selenol groups seems to prevail over metal coordination.¹⁹

Here, we report on the molecular investigation of three organometallic complexes (Figure 1) with model biomolecules by electrospray ionization mass spectrometry (ESI MS), which are compared to related coordination compounds. Compound 1 corresponds to the cyclometalated C,N,N-hydroxido complex

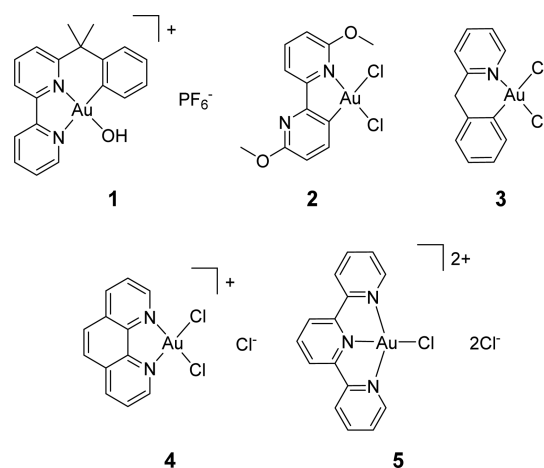


Figure 1. Structures of the gold(III) compounds investigated in this study.

$[Au(bipy^{dmb}-H)(OH)][PF_6]$ ($bipy^{dmb}$ = 6-(1,1-dimethylbenzyl)-2,2'-bipyridine), developed by Cinellu et al. in 2002,²⁵ that is considered stable under pseudophysiological conditions and moderately cytotoxic toward different cancer cell lines sensitive and resistant to cisplatin. Compounds 2 $[Au(bipy^{2OMe}-H)Cl_2]$ ($bipy^{2OMe}$ = 6,6'-dimethoxy-2,2'-bipyridine)²⁶ and 3 $[Au(py^b-H)Cl_2]$ (py^b = 2-benzylpyridine)²⁷ are both C,N-cyclometalated; however, whereas 3 is a normal cyclometalated compound bearing a six-membered ring, 2 is a so-called rollover derivative featuring a five-membered metallacycle. In addition, two classical cytotoxic gold(III) complexes with bidentate or tridentate N-donor ligands, i.e., $[Au(phen)Cl_2]Cl$ ($phen$ = 1,10-phenanthroline; 4)²⁸ and $[Au(terpy)Cl]Cl_2$ ($terpy$ = 2,2';6',2''-terpyridine; 5)²⁹ (Figure 1), were selected to compare their behavior in solution with respect to that of the organometallics.

Thus, 1–5 were studied by ESI MS on ion trap (ESI-IT MS) and time-of-flight (ESI-TOF MS) instruments. ESI-TOF MS is employed because, besides its obvious advantage of higher resolution, it yields higher efficiencies for detecting metal–drug–protein adducts compared to that with IT,³⁰ whereas the latter features MSⁿ options. Consequently, IT MS was used for investigating their stabilities in water and their reactivities toward the natural reducing agent ascorbic acid and toward a mixture of amino acids possessing different nucleophiles. In detail, the compounds were reacted with mixtures of L-histidine (His, imine), L-methionine (Met, thioether), L-cysteine (Cys, thiol), L-glutamic acid (Glu, carboxylic acid), methylseleno-L-cysteine (Se^{Me} -Cys, selenoether), and *in situ* generated seleno-L-cysteine; incubations with amino acids were performed separately without and with Se^{Me} -Cys in order to judge the preference of the gold compounds for binding to the selenoether. The reactivity of the compounds toward the model nucleobase 9-ethylguanine (EtG) and a mixture containing guanosine triphosphate (GTP) and adenosine triphosphate (ATP) was also investigated by ESI-IT MS. Finally, the possible binding of the gold compounds to the model proteins ubiquitin (ub) and cytochrome c (cyt) was studied by ESI-TOF MS. Both cyt c and ub are known to be excellent ESI MS probes and have been the subject of a number of studies aimed at the characterization of the binding of metal compounds with proteins at a molecular level.^{31–36} The obtained results are discussed in relation to the demonstrated inhibition activities of the compounds for the seleno-enzyme

TrxR and in relation to their possible mechanisms of biological (anticancer) action.

RESULTS

Stability in Water and in the Presence of Ascorbic Acid. Initially, the stability of the various gold(III) compounds was studied in aqueous solution (pH ca. 6) by ESI-IT MS monitoring of the sample at different times over 24 h. Incubations were performed at 37 °C, and reaction aliquots were analyzed after 10 min and after 3, 6, and 24 h. Additionally, 1–5 were each exposed to 4 equiv ascorbic acid to evaluate their oxidizing potential, and the reaction was monitored at 10 min and at 3 and 24 h after mixing.

Compound 1 possesses a tridentate C,N,N-cyclometalated ligand and, as expected, shows high stability in water and also in the presence of ascorbic acid over 24 h (Figure S1 in the Supporting Information).

Bis-chloride 2 is C,N-cyclometalated, it hydrolyzes the chlorido ligands relatively fast in water, and an oxo-bridged dimer, corresponding to $[(\text{bipy}^{2\text{OMe}}\text{-H})_2\text{Au}_2(\mu\text{-O})_2 + \text{H}]^+$, is the major species observed after 3 h (Figure S2A in the Supporting Information). In the presence of ascorbic acid, 2 forms exclusively $[(\text{bipy}^{2\text{OMe}}\text{-H})_2\text{Au}^{\text{III}}]^+$ in the mass spectrum within 10 min (Figure S2B in the Supporting Information), which provides indirect evidence that partial reduction of Au^{III} to Au^I or Au⁰ occurs, liberating the bidentate ligand; however, such reduced species were not detected in water. The released ligand can then coordinate to the remaining hydrolyzed $(\text{bipy}^{2\text{OMe}}\text{-H})\text{Au}^{\text{III}}$.

Similar to 2, compound 3 rapidly hydrolyzes the chlorido ligands in water (Figure 2). However, 3 also initially forms a

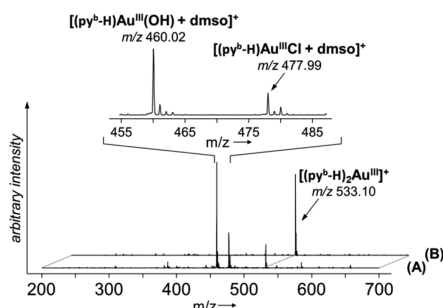


Figure 2. Representative ESI-IT MS spectra of 3 in water (A) and in the presence of 4 equiv of ascorbic acid (B) after a 3 h incubation.

mononuclear dimethyl sulfoxide (DMSO) complex of the form $[(\text{py}^b\text{-H})\text{Au}^{\text{III}}(\text{OH}) + \text{DMSO}]^+$ that converts to $[(\text{py}^b\text{-H})_2\text{Au}^{\text{III}}]^+$ even under nonreducing conditions (without ascorbate). Addition of ascorbic acid led to the rapid and exclusive formation of the $[(\text{py}^b\text{-H})_2\text{Au}^{\text{III}}]^+$ fragment, again supporting partial reduction of the metal center. The transiently observed DMSO adducts are found because stock solutions of 1–5 were prepared in DMSO. The DMSO content is roughly 0.5% after dilution to the final incubation solution. Moreover, DMSO may coordinate via the sulfur or the oxygen, but the interaction with Au^{III} compounds is weak and observed only in the absence of tight or chelate binders, such as amino acids.

Phenanthroline derivative 4 hydrolyzes the Au–Cl bonds and reaches the hydrolysis equilibrium within 3 h in water (Figure S3 in the Supporting Information). Similar to 2 and 3, ligand release and reduction to Au^I is observed; however, it yields a $[(\text{phen})_2\text{Au}^{\text{I}}]^+$ complex in the mass spectrum in which

gold is found in the +1 oxidation state. Terpyridine-containing 5 hydrolyzes within 3 h as well, and reduction to Au^I is underlined by a minor mass signal for free ligand (Figure S4 in the Supporting Information). In the presence of ascorbic acid, the mass signals observed for intact or hydrolyzed 4 and 5 vanished after 10 min, suggesting that the compounds are quickly reduced. Relatively large abundances of free ligand were detected, although, for example, the $[(\text{phen})_2\text{Au}^{\text{I}}]^+$ species could not be observed. Transiently formed mass signals ($z = 2$) of m/z 298.06 and 261.04 for 4 and 5, respectively, could not be assigned to a reasonable structure. Notably, gold-ascorbate adducts were never detected for 1–5.

Interaction with Amino Acids. In order to characterize the interaction of metallodrugs with proteins, it is crucial to investigate binding preferences with amino acids in a competitive experiment. Compounds 1–5 were reacted in an equimolar ratio with amino acid mixtures containing His (imine), Cys (thiol), Met (thioether), and Glu (carboxylic acid) once without and once with Se^{Me}-Cys (selenoether). These amino acids were selected because of their proposed involvement in binding Au^{III} species.^{7,18,21} A list of all of the assigned species in the ESI-IT experiments can be found in Tables S1 and S2 in the Supporting Information. Figure 3 reports the MS spectra of these reactions for compounds 1–3 and highlights the differences between the four amino acid mixture and the seleno-containing mixture. When incubated with the mixture of amino acids, 1 forms predominately

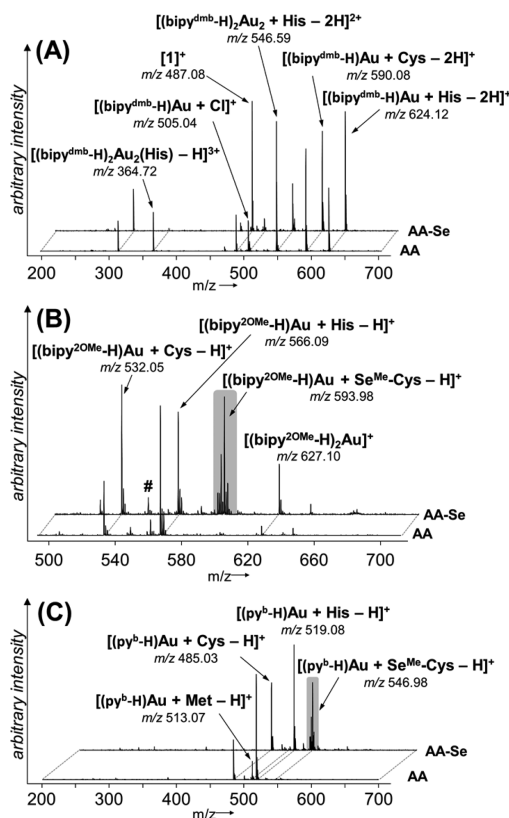


Figure 3. Representative ESI-IT mass spectra for compounds 1 (A), 2 (B), and 3 (C) reacting with amino acid mixtures in the absence (AA) or presence (AA-Se) of Se^{Me}-Cys. Gold-seleno adducts are highlighted in gray. The organometallic Au is always found in the +3 oxidation state. In (B), # corresponds to $[(\text{bipy}^{2\text{OMe}}\text{-H})\text{Au}(\text{Cys}^{\text{ox}}) - \text{H}]^+$ (m/z 548.03).

monomeric Au^{III} adducts with His and Cys and dimeric adducts with His of the type [(bipy^{dm}-H)₂Au₂ + His - 2H]²⁺ via the release of the hydroxido ligand, as shown by ESI-IT MS (Figure 3A). The latter species contains two gold ions in the +3 oxidation state and may represent a histidine bridging two (bipy^{dm}-H)Au^{III} moieties. The mass spectra do not differ significantly over the 24 h incubation period with the exception of a decrease in the signal intensity of dinuclear organogold–histidine adducts, which appear to be only transiently formed. Moreover, intact [1]⁺ is always observed, whereas, interestingly, neither Met nor Se^{Me}-Cys adducts were detected.

Compound 2 forms adducts with His and Cys and to some extent with Met, which correspond to [(bipy^{2OMe}-H)Au^{III}(AA) - H]⁺, where AA is the respective amino acid (Figure 3B). Se^{Me}-Cys adducts were detected upon addition of the selenoether, at the expense of Met adducts. Se^{Me}-Cys resembles Met in structure; however, the seleno-adduct was much more abundant. It appears that oxidation of cysteine occurs to some extent to sulfenic acid or sulfenate, as evidenced from the mass signal at *m/z* 548.03 in the mass spectrum ascribed to [(bipy^{2OMe}-H)Au^{III}(Cys^{ox}) - H]⁺. In parallel, [(bipy^{2OMe}-H)₂Au^{III}]⁺ was also detected during the same incubation, suggesting the reduction of gold(III) by some amino acids. The major interaction products of 3 with the mixture of amino acids correspond to adducts with His and Cys (Figure 3C). In the presence of Se^{Me}-Cys, an intense mass signal appeared corresponding to the respective Se-adduct and was clearly detected after 3 h. The adduct types were of the form [(py^b-H)Au^{III}(AA) - H]⁺, where AA is the respective amino acid, similar to those with 2. The mass spectra did not differ significantly over the entire incubation period for 2 and 3. Additionally, the experimental and simulated isotopic distributions of the seleno-adducts of 2 and 3 are reported in Figure 4, which feature the characteristic isotopic pattern of selenium.

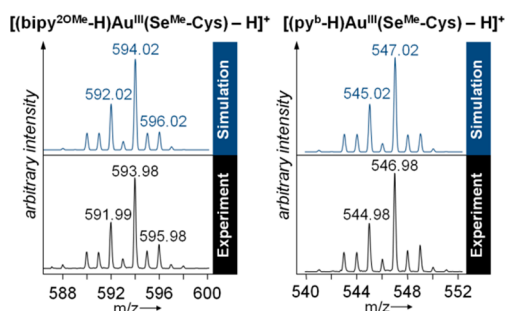


Figure 4. Experimental and simulated isotopic distributions of the seleno-adducts of 2 (left) and 3 (right). In both cases, gold ions are in the +3 oxidation state.

Interestingly, coordination compounds 4 and 5 both showed very similar mass spectra when reacted with amino acids compared to the spectra from the reaction with ascorbic acid and the free ligands, and the unidentified mass signals of *m/z* 298.06 and 261.04 were again detected. Remarkably, amino acid adducts with gold were not observed in the presence or absence of the selenoether. However, for both 4 and 5, a mass signal at *m/z* 241.02 was detected, suggesting the formation of cysteine ($m_{\text{theor}} = 241.03$).

In addition to the ESI-IT MS measurements, the samples of 1–5 incubated for 24 h with the mixture of amino acids containing Se^{Me}-Cys was analyzed on the high-resolution TOF instrument, i.e., identical samples were measured under very

similar spraying conditions. Importantly, the TOF experiments were performed using a declustering potential of 8 eV that was not applied on the IT instrument. The general trends were very similar compared to those from the ESI-IT measurements. Again, 1 did not form Se^{Me}-Cys adducts, and the intact complex was mainly observed along with a Cys adduct. Interestingly, His adducts were not observed at all on the TOF instrument. Compounds 2 and 3 formed identical adducts compared to those observed with ESI-IT but featured an additional selenium mass signal corresponding to [LAu^{III} + SeCH₃]⁺, where L = (bipy^{2OMe}-H) or (py^b-H) (Figures S5 and S6 in the Supporting Information). The species were positively identified with an accuracy of <5 Δppm and underline the direct binding of organometallic Au^{III} to selenium (Table 1). The Δppm designates the deviation of the accurate (measured) mass from the exact (theoretical) mass of a given ion in parts per million. A given ion is positively identified with high confidence if Δppm is <5. Surprisingly, the [LAu^{III} + SeCH₃]⁺ species, where L = (bipy^{2OMe}-H) or (py^b-H), were observed at low abundance on the TOF instrument, but they were absent in the IT mass spectra.

Moreover, complexes 4 and 5 did not reveal any mass signals assignable to amino acid adducts except for the unidentified mass signals that were already observed on the IT instrument, but cystine was again detected in small amounts ($m_{\text{acc}} = 241.0310$, $m_{\text{ex}} = 241.0311$) for both 4 and 5, underlining that these compounds indeed oxidize the thiolate of cysteine upon their own reduction (Figure S7 in the Supporting Information). Other oxidation products of His, Met, or Cys were not observed, which may be due to the relatively high pH of 6 of the reaction solution compared to that of the acidic milieu of previous investigations.¹⁸ The pH of the solution of our studies specifically addresses the effect of tumor-related acidity as it is known that solid tumors may acidify to approximately pH 6.5.³⁷

Interaction with Selenocysteine (Se-Cys). As previously mentioned, gold compounds were shown to behave as potent inhibitors of the seleno-enzyme TrxR via a mechanism that most likely involves direct binding of Au ions to the seleno-enzyme's active site. Thus, we directly analyzed the interactions of compounds 1–5 with seleno-L-cysteine (Se-Cys) using ESI MS by adapting previously reported procedures.²³ Se-Cys is produced *in situ* from selenocystine in the presence of 4 equiv of dithiothreitol (DTT). The incubation mixture therefore contains Se-Cys, DTT, and oxidized DTT in addition to the gold complex. It is worth mentioning that Se-Cys displays a selenol group, whereas DTT has two thiols; therefore, these functional groups are expected to be the most efficient reagents to bind to the gold compounds under investigation. The obtained results are presented in Figure 5, and the list of experimental (*m/z*) and theoretical (m_{theor}) mass signals attributed to each of the species during the ESI-IT MS experiments of 1–5 with selenocysteine is reported in Table 2.

The MS analysis of this reaction mixture shows that Au(N,N,C) complex 1 forms mainly Se-Cys adducts and only very minor amounts of DTT adducts. Intact [1]⁺ was not detected, but the mass spectra feature signals corresponding to selenocystine and free (bipy^{dm}-H). The free ligand is an indication that even this well-stabilized Au^{III} center may be partially reduced under these conditions. It is believed that reduction leads to a loss of the square-planar geometry and ligand release. However, Au^I compounds were not detected. An additional mass signal was detected at *m/z* 442.04 that features an isotopic distribution characteristic for selenium. The mass

Table 1. Accurate (m_{acc}) and Exact Masses (m_{ex}) of the Detected Species during High-Resolution ESI-TOF MS Experiments of the Incubations Containing Amino Acids^a

compound	species	m_{acc}	m_{ex}	Δppm
amino acid related	(Glu + H) ⁺	148.0606	148.0604	1.4
	(Met + H) ⁺	150.0588	150.0583	3.3
	(His + H) ⁺	156.0771	156.0767	2.6
	(cystine + H) ⁺	241.0310	241.0311	0.4
1	[1] ⁺	487.1091	487.1079	2.5
	[(bipy ^{dmb} -H)Au ^{III} + Cys - 2H] ⁺	590.1183	590.1171	2.0
2	[(bipy ^{2OMe} -H)Au ^{III} + SeCH ₃] ⁺	506.9896	506.9881	3.0
	[(bipy ^{2OMe} -H)Au ^{III} + Cys - 2H] ⁺	532.0610	532.0600	1.9
	[(bipy ^{2OMe} -H)Au ^{III} + Cys ^{ox} - 2H] ⁺	548.0525	548.0549	4.4
	[(bipy ^{2OMe} -H)Au ^{III} + His - 2H] ⁺	566.1110	566.1097	2.3
	[(bipy ^{2OMe} -H)Au ^{III} + Se ^{Me} -Cys - H] ⁺	594.0214	594.0202	2.0
3	[(py ^b -H)Au ^{III} + SeCH ₃] ⁺	459.9889	459.9874	3.3
	[(py ^b -H)Au ^{III} + Cys - 2H] ⁺	485.0605	485.0593	2.5
	[(py ^b -H)Au ^{III} + His - 2H] ⁺	519.1103	519.1090	2.5
	[(py ^b -H)Au ^{III} + Se ^{Me} -Cys - H] ⁺	547.0211	547.0194	3.1
4	(phen + H) ⁺	181.0758	181.0760	1.1
	n.a.	298.0701		
5	(terpy + H) ⁺	234.1030	234.1026	1.7
	n.a.	261.0627		

^aThe accuracy of the mass signals is expressed as the deviation in parts per million (Δppm).

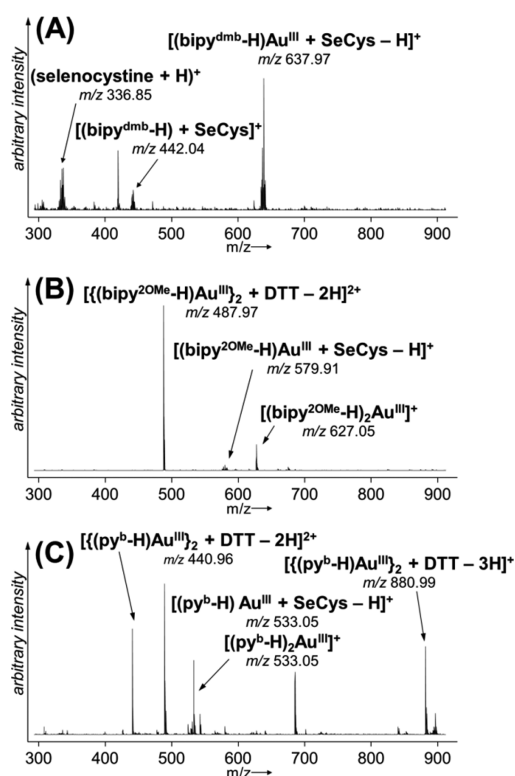


Figure 5. Representative ESI-IT mass spectra for compounds 1 (A), 2 (B), and 3 (C) reacting with *in situ* generated selenocysteine (Se-Cys) from selenocysteine and an excess of dithiothreitol (DTT). The organometallic Au is always found in the +3 oxidation state.

difference between this signal and the signal of the gold-Se-Cys adduct is 195.92 Da, corresponding to Au. This indicates that the lower mass signal may be due to an adduct between (bipy^{dmb}-H) and Se-Cys. The mass signals remained relatively constant over the entire incubation period for all compounds.

Table 2. Experimental (m/z) and Theoretical (m_{theor}) Mass Signals Attributed to Each Species during ESI-IT MS Experiments of Compounds 1–5 with Se-Cys^a

species	m/z	m_{theor}
(bipy ^{dmb} + H) ⁺	274.42	274.15
(selenocystine + H) ⁺	336.85	336.92
(bipy ^{dmb} + Se-Cys + H) ⁺	442.04	442.10
[(bipy ^{dmb} -H)Au ^{III} + DTT - H] ⁺	623.02	623.11
[(bipy ^{dmb} -H)Au ^{III} + Se-Cys - H] ⁺	637.97	638.06
[{(bipy ^{2OMe} -H)Au ^{III} } ₂ + DTT - 2H] ²⁺	487.97	488.05
[(bipy ^{2OMe} -H)Au ^{III} + Se-Cys - H] ⁺	579.91	580.00
[(bipy ^{2OMe} -H) ₂ Au ^{III}] ⁺	627.05	627.13
[{(bipy ^{2OMe} -H)Au ^{III} } ₂ + DTT - 3H] ²⁺	974.96	975.09
[{(py ^b -H)Au ^{III} } ₂ + DTT - 2H] ²⁺	440.96	441.04
[(py ^b -H)Au ^{III} Cl + DMSO] ⁺	477.95	478.03
[(py ^b -H)Au ^{III} + Se-Cys - H] ⁺	533.05	533.00
[(py ^b -H) ₂ Au ^{III}] ⁺	533.05	533.13
[{(py ^b -H)Au ^{III} } ₂ + DTT - 3H] ²⁺	880.99	881.08
[{(py ^b -H)Au ^{III} } ₂ + Se-Cys - 2H] ²⁺	895.93	896.04

^aAll experimental mass signals include a standard deviation of $m/z \pm 0.05$.

Compound 2 reacted with the Se-Cys/DTT mixture in a similar manner as that of the other amino acids and mainly forms dinuclear species containing a bridging DTT or Se-Cys. Moreover, partial reduction of the metal is indicated by the presence of [(bipy^{2OMe}-H)₂Au^{III}]⁺. Again, intact [2]⁺ was not detected. In contrast to 1, compound 2 seems to interact preferentially with the thiols of DTT and not with the selenol. Excerpts of the ESI-IT mass spectra displaying the isotopic distribution of the seleno-adducts of 1 and 2 are presented in Figure 6.

Complex 3 formed similar reaction products to those formed with 2, and dinuclear species containing DTT or Se-Cys were detected, as were bis-chelated species [(py^b-H)₂Au^{III}]⁺ (m/z 533.05, $m_{\text{theor}} = 533.00$), indicative of partial reduction of the gold(III) center. A mononuclear adduct of the type [(py^b-

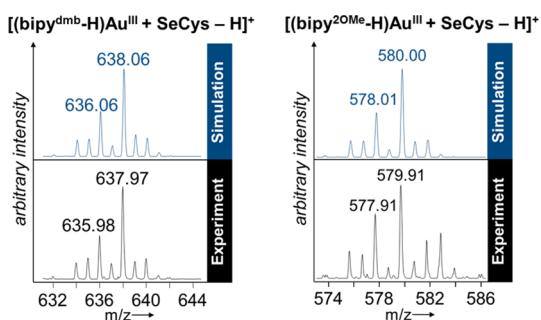


Figure 6. Excerpts of the ESI-IT mass spectra of Figure 5 displaying an isotopic distribution of the seleno-adducts of **1** (left) and **2** (right).

H)Au^{III} + Se-Cys – H]⁺ was also detected. Compound **3** reacts preferentially with DTT and not with Se-Cys, similar to **2**. In contrast to the organometallic Au^{III} compounds of this series, coordination compounds did not show any mass signal attributable to a gold-seleno adduct. It seems that **4** and **5** are rapidly decomposed by redox reactions, and stable intermediates were not detected. Consequently, the following trend of stable adduct formation with Se-Cys is proposed: **1** > **3** > **2** > **4** = **5**.

Interaction with 9-Ethylguanine. Compounds **1–5** were reacted with 2 equiv of EtG, which serves as a nonionic DNA model and as a proof-of-principle regarding whether these compounds form DNA adducts. Compound **1** reacts readily with EtG by hydrolyzing the hydroxido ligand and forming an EtG adduct corresponding to [(bipy^{dm}b-H)Au^{III}(EtG) – H]⁺, most probably via coordination to guanine-N7 (Figure S8). The adduct is observed after 10 min and remains constant over 24 h, which suggests fairly fast hydrolysis and reaction kinetics. Organometallic compounds **2** and **3** show only very minor mass signals for EtG adducts even after 24 h, which are, however, of the same type as those found for **1**, i.e., only monoadducts were observed with Au in the +3 oxidation state (data not shown). Readily detectable EtG adducts were observed for **4** and **5** upon hydrolysis of the Au–Cl bonds (Figure 7A). The EtG adducts of the form [LAu^{III}(EtG) –

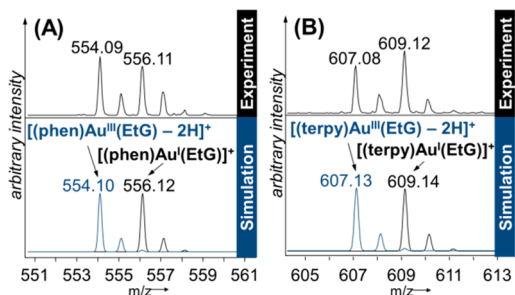


Figure 7. Excerpts of ESI-IT mass spectra of **4** (A) and **5** (B), which were reacted with 2 equiv of EtG for 24 h, featuring characteristic Au^I/Au^{III} pairs. The experimental and simulated signals are shown.

2H]⁺ increase over time for **4** but remain constant for **5**. Interestingly, both **4** and **5** show mass signals of Au^I/Au^{III} couples, which were not observed for organometallic derivatives **1–3** (Figure 7B).

Interaction with Nucleotides. Following the experiments with EtG, the five compounds were exposed to an equimolar mixture (1:1:1) of guanosine triphosphate (GTP) and adenosine triphosphate (ATP). The nucleotides were used to

evaluate the additional negative charge of the phosphates and the possible preference for specific nucleobases. The mass spectra of these experiments were recorded in negative ion mode. Initially, the blank mixture of GTP and ATP was recorded at different time intervals and did not change significantly over 2 weeks at room temperature. Several mass signals were observed corresponding to ATP, GTP, adenosine diphosphate (ADP), and guanosine diphosphate (GDP), including their mono- and disodium adducts (Figure S9 in the Supporting Information). Reducing the temperature of the dry gas to 120 °C and the capillary voltage to ±3 kV did not significantly reduce the signals for ADP and GDP, which were unexpectedly found. This suggests that the diphosphates are present in solution and are not a product of an in-source fragmentation reaction.

Organometallics **1–3** formed nucleotide adducts to similar extents and were fairly abundant (Figure 8), whereas **4** formed adducts to a very minor extent. Interestingly, **5** did not form any adducts with either GTP or ATP.

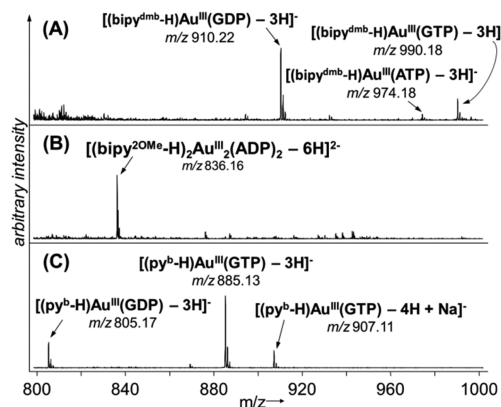


Figure 8. Compilation of ESI-IT mass spectra recorded for **1** (A), **2** (B), and **3** (C), which were reacted with an equimolar mixture of GTP and ATP for 24 h. The spectra were recorded in negative ion mode. All Au species are present in the +3 oxidation state.

In detail, **1** formed GTP/GDP and ATP adducts, corresponding to [(bipy^{dm}b-H)Au(NP) – 3H][–], where NP is the respective nucleotide (Figure 8A). These adducts remained constant over time, and a preference for GTP over ATP was observed. The positive ion mode featured [I]⁺ as the unique mass signal and indicates that it does not react quantitatively with the GTP/ATP mixture.

In the case of **2**, owing to subsequent hydrolysis processes of the compound that led to substitution of the chlorido ligands with water/hydroxo molecules, the intensities of the adducts with nucleotides increased over time (Figure 8B). Compound **2** interacted preferentially with ATP/ADP over GTP and again formed dimetallic adducts, e.g., [(bipy^{2OMe}-H)₂Au^{III}₂(ATP)₂ – 7H]^{3–}, which is probably symmetrically ATP-bridged (see also Figure S10 in the Supporting Information for the lower mass range). Even a mixed ATP/ADP species (*z* = –3) was observed at *m/z* 583.74. Compound **3** formed mainly GTP/GDP adducts, similar to **1** (Figure 8C).

Complex **4** formed nucleotide adducts only to a very minor extent (Figure S11 in the Supporting Information), which corresponded to GTP/GDP adducts of the type [(phen)-Au^{III}(NP) – 4H][–], and these slightly increased over time, similar to **2**. Notably, the detection of a hydroxido complex

corresponding to $[(\text{phen})\text{Au}^{\text{III}}(\text{NP})(\text{OH}) - 3\text{H}]^-$ and again a $\text{Au}^{\text{I}}/\text{Au}^{\text{III}}$ redox couple were observed at m/z 896–898. According to the redox couple of 4 with nucleotides and the concomitant detection of Au^{I} , free-ligand species corresponding to $[\text{phen} + \text{H}]^+$ (m/z 181.05, $m_{\text{theor}} = 181.09$) and $[\text{terpy} + \text{H}]^+$ (m/z 234.09, $m_{\text{theor}} = 234.10$) were observed in the positive ion mode of 4 and 5, respectively, in these incubations (data not shown).

Additionally, the guanosine/adenosine (G/A) ratios and diphosphate/triphosphate ratios were determined from the relative intensities of the detected metal-nucleotide adducts. It is assumed that the ionization efficiencies are similar for the G/A and diphosphate/triphosphate pairs. In the GTP/ATP blank without gold, the G/A ratio was 0.3 and the ratio of nucleotide diphosphates to nucleotide triphosphates was 10. Compounds 1, 3, and 4 preferred guanosine over adenosine with blank-normalized ratios of >30 . The blank normalization showed that organometallic 2 did not show any preference for one nucleotide over the other. Interestingly, the preference for guanosine by 1, 3, and 4 is paralleled by an increased affinity for the diphosphate over the triphosphate. Compound 2 was indiscriminate with respect to the nucleobase, but it largely preferred triphosphates over diphosphates (Table S2).

Interaction with Proteins. In a last series of experiments, compounds 1–5 were incubated separately with ub and cyt at a 2:1 metal-to-protein ratio for 24 h at 37 °C, and the samples were analyzed by ESI-QTOF MS. It has been shown that TOF instruments yield higher efficiencies for detecting metallodrug–protein adducts compared to that using IT instruments.³⁰ Compound 1 did not form any adducts with either ub or cyt during the incubation period, although in the previously discussed experiments with mixtures of single amino acids it could form adducts with His and Cys.

Conversely, 2 and 3 formed mono- and bis-adducts of the type $[\text{protein} + n\text{LAu}^{\text{III}}]^+$, where L is the respective C,N-bidentate ligand and $n = 1$ or 2, with both proteins to a similar extent (Figures 9 and S12). A list of all of the detected protein

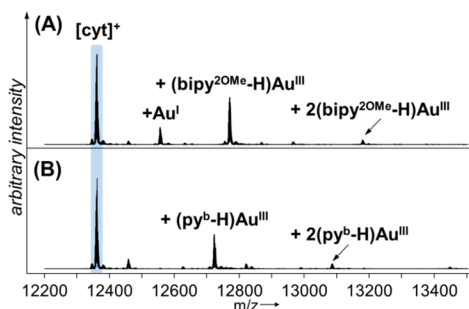


Figure 9. Compilation of deconvoluted ESI-QTOF mass spectra for compounds 2 (A) and 3 (B) incubated with cyt for 24 h at 37 °C (Au/protein ratio = 2:1).

adducts is displayed in Table S3. Interestingly, the mixture containing 2 displayed an additional adduct corresponding to $[\text{cyt} + \text{Au}^{\text{I}}]^+$ (Figure 9A). This is in accordance with the previous experiments of 2 incubated with the amino acids, where reduction of the metal center was shown indirectly by the formation of $[(\text{bipy}^{2\text{OMe}}\text{-H})_2\text{Au}^{\text{III}}]^+$. Indeed, the latter species was also detectable in the full mass spectrum of the protein incubation in the absence of ascorbic acid. Notably, 3 did not feature such Au^{I} species in the deconvoluted spectrum,

but $[(\text{py}^{\text{b}}\text{-H})_2\text{Au}^{\text{III}}]^+$ ions were detected in the full mass spectrum.

Complexes 4 and 5 reacted similarly with both proteins by extensively forming adducts and also higher order adducts with exclusively Au^{I} and $\text{Au}^{\text{I}}\text{Cl}$ moieties, e.g., adducts up to $[\text{cyt} + 3\text{Au}^{\text{I}} + 2\text{Cl}]^+$ were observed for 5 (Figure 10). It is interesting

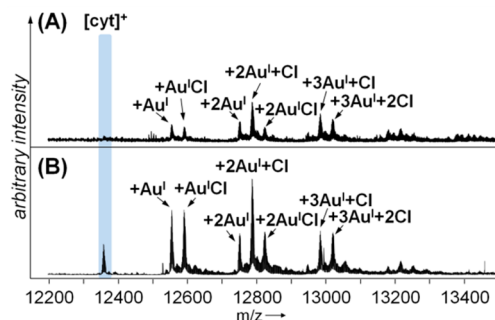


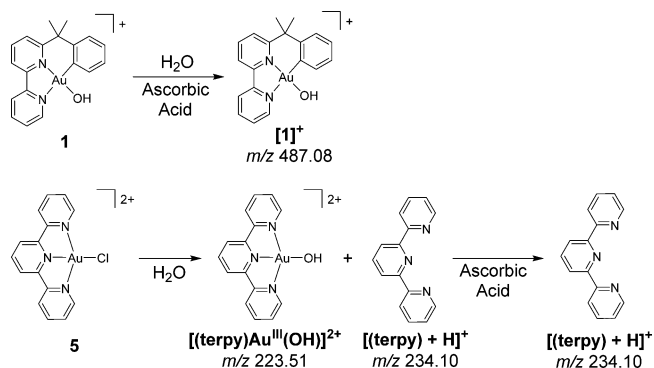
Figure 10. Compilation of deconvoluted ESI-QTOF mass spectra for compounds 4 (A) and 5 (B) incubated with cyt for 24 h at 37 °C (Au/protein ratio = 2:1).

to note that both complexes undergo reduction and ligand release. Moreover, gold complexes 4 and 5 form adducts with cyt to a greater extent compared to those with 2 and 3. Cyt bears a heme B cofactor with redox properties and underlines further the redox sensitivities of 4 and 5.

DISCUSSION

Stability and Possible Activation Pathways in Aqueous Solution. Investigating the stability and ligand-exchange reactions of putative metallodrugs is important for their further design and development. ESI-MS is ideally suited for this purpose because the m/z information allows conclusions on molecular composition and even structure to be directly drawn.³⁸ The obtained ESI-MS data for the stability of 1–5 in water allowed us to construct the reaction pathways summarized in Schemes 1 and 2. The reactivity of the Au^{III}

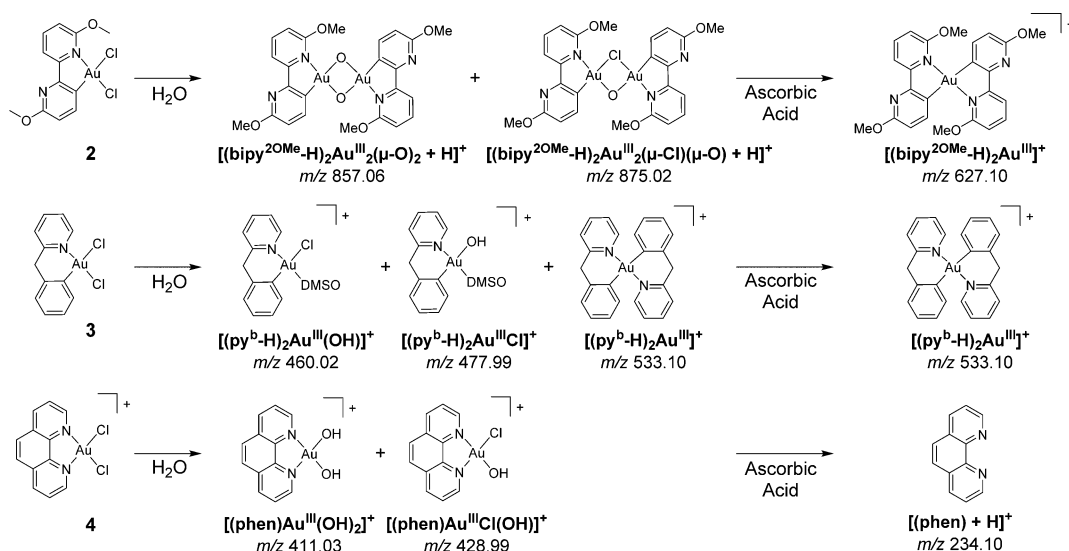
Scheme 1. Stability in Water and Reactivity in the Presence of 4 Equiv of Ascorbic Acid of Au^{III} Compounds 1 and 5 with Tridentate Ligands



compounds in the presence of ascorbic acid was additionally investigated because of their oxidizing character and to characterize reaction products owing to possible metal reduction.

On the basis of these results, the cyclometalated hydroxo complex 1, featuring a terdentate C,N,N ligand, is stable in

Scheme 2. Stability in Water and Reactivity in the Presence of 4 Equiv of Ascorbic Acid of Au^{III} Compounds 2–4 with Bidentate Ligands



water and is not reduced even in the presence of 4 equiv of ascorbic acid over 24 h (Scheme 1). The cation of intact **1** is the only mass signal observed. The cyclometalated complex **2**, bearing a bidentate C,N ligand and two hydrolyzable chlorido ligands, forms a dinuclear oxo-bridged gold(III) species in water, an already known synthetic motif in the field of gold metallodrugs (Scheme 2).³⁹ This dimer is stable in aqueous solution. In contrast to **1**, complex **2** is reduced by ascorbic acid, as evidenced by the observation of the bis-cyclometalated species $[(\text{bipy}^{2\text{OMe}}\text{-H})_2\text{Au}^{\text{III}}]^+$ in solution. Such bis-cyclometalated complexes have been previously obtained after electrochemical reduction of both $[\text{Au}(\text{C,N})\text{Cl}_2]$ and $[\text{Au}(\text{C,N,N})\text{Cl}]^+$ complexes as a result of the partial reduction of the Au^{III} center to Au⁰ followed by a transcyclometalation process, but they were difficult to observe by chemical reduction.⁴⁰ Compound **3** also undergoes hydrolysis of the chlorido ligands, but the compound remains mononuclear, whereas DMSO from the stock solution seems to coordinate to the hydrolyzed species, which was not observed for any other compound of this series, although all of the compounds were initially dissolved in DMSO. Moreover, **3** is reduced to some extent even in purely aqueous solution to produce $[(\text{py}^{\text{b}}\text{-H})_2\text{Au}^{\text{III}}]^+$ species, indicating an increased tendency for reduction compared to that of **2**. The lower stability of **3** is in accordance with the chelating ligand py^{b} forming a six-membered cycle with the metal compared to that of **2**, which features a five-membered cycle. It is an interesting fact that both **2** and **3** form similar and very stable $[\text{L}_2\text{Au}^{\text{III}}]^+$ species, where L is either $(\text{bipy}^{2\text{OMe}}\text{-H})$ or $(\text{py}^{\text{b}}\text{-H})$, respectively, which represent our marker for reduction processes. However, their formation in an environment such as blood plasma or the cell interior seems improbable due to the abundance of other nucleophiles with which the gold compounds may associate.

Coordination compounds **4** and **5** rapidly hydrolyze in water and are quickly reduced, which results in ligand loss and the detection of free ligands in the mass spectra. It is worth mentioning that gold reduction in these cases was only indirectly observed by monitoring the increase of the free ligands in the mass spectra, whereas Au^I ions were hardly directly detected, with the exception of $[(\text{phen})_2\text{Au}^{\text{I}}]^+$, suggesting possible reduction to Au⁰.

Overall, the ESI MS data of the interaction with ascorbic acid confirms that organometallic C,N- and C,N,N-type gold(III) organometallics are more stable with respect to reduction and ligand loss compared to that of the related coordination compounds with purely N-donor ligands. For example, **1** remains stable over the entire incubation period, but **5** is quickly reduced and free terpy is detected. A clear increase in redox stability of the organometallic compounds was determined to follow the order six-membered C,N-metallacycle **3** < five-membered C,N-metallacycle **2** < five- and six-membered C,N,N-metallacycle **1**.

Interactions with Mixtures of Amino Acids. As a result of their different redox and nucleophilic properties, the gold(III) complexes manifest different reactivities with amino acids. The compounds were separately incubated with Se-Cys/DTT (1:2:4) and Glu/His/Met/Cys/Se^{Me}-Cys mixtures (1:1:1:1:1) in a competitive manner. The former incubation includes selenols and thiols as the main functional groups, and the latter includes thiols, selenoether, thioether, imines, and carboxylates. The two separate reactions may allow the preferred binding affinities to certain amino acids to be elaborated and may have relevance to their potency of TrxR inhibition.

Concerning the reactivity with Se-Cys and DTT, the obtained ESI-IT MS data suggests that the compounds react with Se-Cys in the following order: **1** > **3** > **2** \gg **4** and **5**. Compound **1** reacts exclusively with Se-Cys, forming an adduct of the type $[(\text{bipy}^{\text{dmb}}\text{-H})\text{Au}^{\text{III}}(\text{Se-Cys}) - \text{H}]^+$. Compounds **2** and **3** form similar adducts with Se-Cys, but they do so to a lower extent; additionally, DTT adducts are very prominent in the mass spectra for these two compounds. The higher reactivity toward Se-Cys of **3** compared to that of **2** is highlighted by comparing the intensity ratios of the gold-Se-Cys over the gold-DTT adduct and amounts to 20 and 3% for **3** and **2**, respectively. In both cases, dimetallic DTT adducts were detected with two Au^{III} centers and one potentially bridging DTT. The presence of DTT also seems to lead to partial reduction of the metal, as evidenced by the characteristic markers for reduction, i.e., $[\text{L}_2\text{Au}^{\text{III}}]^+$ species. Strikingly, compounds **4** and **5** did not show any adducts with an isotopic pattern containing selenium. When reacted with the amino acid

mixture containing Glu/His/Met/Cys/Se^{Me}-Cys, compounds **2** and **3** extensively formed adducts with methylselenocysteine, whereas none of the other compounds did. Methylselenocysteine (selenoether) is a homologue of methionine. However, methionine adducts were observed only for **3** in low abundance in the absence of Se^{Me}-Cys, but they vanished in the presence of the seleno-ether, indicating a selective interaction with selenium over sulfur. Additionally, His and Cys adducts were observed for the two C,N-containing compounds. It seems that these gold-seleno-adducts are especially favored when a bidentate C,N-cyclometalated ligand is bound to Au^{III}. Under these conditions, **1** showed a preference for His and Cys, but it did not display seleno-ether adducts.

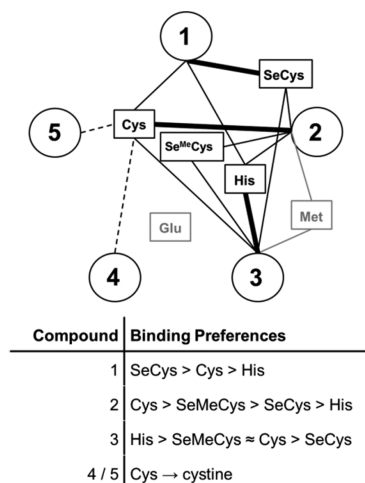
The mixture of amino acids was able to induce reduction of **2** to some extent. Finally, we did not detect any adducts between Au^{III} or Au^I and amino acids in the mass spectra of **4** or **5**. However, particularly with the latter two compounds, ESI-IT and -TOF MS experiments showed the formation of cystine, which stems from Au-mediated oxidation of cysteine thiolates and parallels previous findings for Au^{III} coordination compounds interacting with Cys.¹⁸

The experiments on the QTOF instrument were carried out under an 8 eV collision energy to aid in declustering the solvent from analyte molecules. This additional energy, however, resulted in two main differences compared to the ESI-IT measurements. First, the His adducts of **1** vanished completely, yielding only a Cys adduct (Figure S5 in the Supporting Information). Consequently, experiments with a slightly increased energy in the mass spectrometer underline that the interaction between **1** and His is weak and that the interaction with Cys is favored. Second, it was possible to detect methyl selenolate adducts for **2** and **3**. The observation of these adducts indicates partial activation of the seleno-ether upon direct Au^{III} coordination to the selenium atom and easily undergoes fragmentation reactions when a low declustering potential is applied.

Integrating these results for **1**–**5** with amino acids yields a small network, as depicted in Scheme 3. Each circle represents a Au^{III} compound of this series, and each connection represents a detected adduct. Gray boxes denote amino acids that were not observed in the presence of a selenium-containing amino acid, e.g., adducts between gold and Glu were not observed. The dashed lines of **4** and **5** indicate a reaction with Cys because cystine was observed; however, it was not possible to directly prove the formation of any gold-adduct by MS. Thick lines indicate the preferred binding partner of the respective Au^{III} compound. Consequently, compound **1** is selective for Se-Cys, **2** is selective for Cys, and **3** is mostly selective for His. The binding preferences of **1** and **3** for amino acids are quite opposed.

Interactions with Proteins. As we have often reported in past years, the reactivity of compounds with proteins may be influenced not only by the presence of certain suitable binding sites for metal compounds but also by the overall protein sequence/folding, isoelectric point, the presence of charged surfaces, or even the method itself.^{30,41–44} Therefore, we tested the compounds of this series on two proteins of different families, namely, cyt c, a small electron-carrier heme protein localized in the mitochondria that plays a crucial role in apoptotic pathways, and ub, which is relevant in post-translational modification of proteins together with the proteasome system. Both cyt c and ub are of small to moderate size, with molecular masses of 12.3 and 8.6 kDa, respectively.

Scheme 3. Interaction Network of Compounds **1**–**5** with the Tested Amino Acids and Preferences for Adduct Formation with Single Amino Acids^a



^aCircles denote Au^{III} compounds, boxes denote amino acids, straight lines indicate detected Au^{III}-amino acid adducts, and dashed lines indicate indirect evidence for interaction. Gray boxes and lines indicate Au^{III}-amino acid adducts that were not observed in the presence of a selenium-containing amino acid but may form in the absence of selenium amino acids.

They are commercially available, manifest a high stability in solution under physiological-type conditions, and are water-soluble. In most cases, they are easily ionizable and optimal for ESI MS detection in positive ion mode. In addition, for both of these proteins, high-resolution crystal structures or NMR structural data are available, complementing the identification of the probable metal binding sites (e.g., the most surface-exposed residues). Both proteins have also a few free sites that are available and surface exposed that may specifically react with transition metal ions. For example, platinum and ruthenium anticancer drugs have been proven to react with His26, His33, and Met65 in cyt c and with Met1 and His68 in ub, with a preference for S-donor residues.^{32–35,45}

According to our results, complex **1** does not form any adduct with either model protein under the applied reaction conditions. This is not fully in accordance with what has been previously reported for the interaction of the dinuclear oxo-bridged analogue of **1** with cyt c, as studied by high-resolution LTQ-Orbitrap ESI MS.¹⁹ In that case, the dinuclear μ -oxo complex formed both mono- and bis-adducts containing [Au^{III}(bipy^{dmb}-H)]²⁺ fragments. This is most probably due to the use of a dinuclear compound as the starting material, which doubles the presence of Au^{III}-reactive moieties upon dissociation with respect to **1**. It is also worth mentioning that an X-ray crystallographic study on the interaction of **1** with the model protein lysozyme showed that a Au^I ion binds to the side chain of a Gln residue.⁴⁶ It must be pointed out that the crystallization conditions used ethylene glycol, which may be responsible for the reduction of the Au^{III} compound, thus allowing the terdentate ligand to detach. Nonetheless, this is a further indication that the proteins are able to prevent a complete reduction to Au⁰.

Compounds **2** and **3** form Au^{III} mono- and bis-adducts after a 24 h incubation with both proteins. The adducts are of the type [n(LAu^{III}) + protein], where n = 1 or 2 and L is the respective C,N ligand. Notably, a Au^I adduct was detected upon

incubating **2** with cyt but not with ub, indicating the redox properties of the heme-containing protein. Interestingly, in the case of complex **2**, the presence of the bis-cyclometalated species $[(\text{bipy}^{2\text{OMe}}\text{-H})_2\text{Au}^{\text{III}}]^+$ in the full mass spectrum is indirectly indicative of reduction, whereas the analogous species is not observed for **3**. Therefore, cyt binding may reduce the susceptibility of **3** for reduction.

Our results further support the idea that **4** and **5** are very susceptible to reduction because they form only Au^{I} - and $\text{Au}^{\text{I}}\text{Cl}$ -type adducts with the selected model proteins. It is assumed that these N-donor ligands facilitate the reduction to Au^{I} and are then released from the metal because of the change in the coordination mode. Interestingly, we also find that the proteins help to stabilize the Au^{I} species in general, which were hardly detected during the experiments with mixtures of single amino acids.

Relation to the Inhibitory Effects on TrxR1 and Antiproliferative Activity. In order to validate the reactivity patterns obtained by the mass spectrometric experiments, we compared our data with the inhibitory potency of **1–4** on thioredoxin reductase 1 (TrxR1). Remarkably, for organometallics **1–3**, the extent of forming Se-Cys adducts is in perfect accordance with their inhibitory effects against the seleno-enzyme TrxR1 (Table S4). Therefore, the model interactions with Se-Cys appear to reflect well the interaction with TrxR1. Moreover, **4** appears to inhibit TrxR1 to a certain extent as well; however, previously reported data on similar gold(III) coordination complexes with N-donor ligands suggest that protein inhibition may occur via progressive oxidative damage of thiol groups (Cys) in the protein's side chains.¹⁹ Intriguingly, the same extends to the antiproliferative effects on human ovarian cancer cell lines for **1–4** (A2780 cells; Table S4). Compounds **1** and **4** are the most potent inhibitors of TrxR1 and also show the highest antiproliferative effect with activities in the low micromolar range. They are then followed by **3** and finally by **2**, showing the lowest activities. Additionally, ligand release of N-donor-containing complexes such as phen and terpy must be considered because of the toxicity of the free ligand itself that also affects cell viability in *in vitro* assays.

It is also worth mentioning that **1–3** form stable adducts with amino acids and proteins while at the same time retaining their ligands and are selective for certain side chains, which does not seem to be the case for **4** and **5**. Instead, the latter are quickly reduced, inducing ligand release, and adducts with amino acid were not observed, whereas $\text{Au}^{\text{I}}\text{Cl}$ adducts were observed with proteins. Thus, it appears that the molecular mechanisms of action of the organometallic gold(III) compounds are very distinct from those of the coordination compounds. Notably, **4** has been shown to interact with the zinc finger domain of the protein poly(adenosine diphosphate (ADP)-ribose) polymerase 1 and other model zinc fingers.^{47,48} Interestingly, high-resolution ESI Orbitrap FT-MS showed that **4** binds to the zinc finger domains via substitution of the Zn^{2+} ion, with subsequent formation of a gold finger, in which Au ions remain in the +3 oxidation state.

Interactions with DNA Model Compounds. For several years, nucleic acids have been the subject of intense investigation as the only targets for metallodrugs, and mass spectrometric methods are well-established for investigating these interactions.^{49–52} It was only during the past decade that protein targets were considered for metallodrugs.³⁸ Earlier investigations showed that gold compounds are, in general, poorly reactive toward nucleic acids. All tested compounds of

this series were able to form adducts with EtG, as well as GTP and ATP, with the exception for **5** $[\text{Au}(\text{terpy})\text{Cl}]\text{Cl}_2$, which forms adducts only with EtG. In contrast to the interaction with amino acids, adduct formation with nucleotides did not induce phenanthroline release in **4**, which is probably related to the absence of a strong chelating effect or reductive force. Interestingly, the selected gold compounds preferred guanosine over adenosine (blank-normalized G/A ratio of adduct formation for **1**, **3**, and **4** was clear-cut, >30), with the exception of **2**, which was indiscriminate, and of **5**, for which nucleotide adducts were not detected. This suggests that the ligand may also play a role in determining the selectivity toward a nucleotide type. Additionally, the preference for guanosine seems to be accompanied by a preference for guanosine triphosphate over guanosine diphosphate, which may be explained by enhanced electrostatic interactions of the negatively charged nucleotide and the positively charged gold compounds. Overall, organometallics **1–3** are all more reactive toward nucleobases compared to that of coordination compounds **4** and **5** while at the same time being more resistant to reduction, which allows for a higher efficiency of adduct detection.

Although the extent of binding to nucleotides is lower compared to that for amino acids or proteins, the ability to interact with DNA offers potential alternative pathways for exerting biological effects that may be explored in more detail. It is worth mentioning that Rubbiani et al. recently investigated the interactions of C,N-cyclometalated Au^{III} complexes with guanosine monophosphate by ¹H NMR and showed that after a 24 h incubation interactions between the gold compounds and the model nucleoside take place, which is in accordance with our findings by ESI-MS.⁵³

CONCLUSIONS

Mass spectrometry has emerged as an important tool for studying anticancer metallodrugs in complex biological samples and for characterizing their interactions with biomolecules and potential targets on a molecular level. Here, we exploited ESI MS to elaborate the molecular reactivity of coordination and organometallic gold(III) drug candidates using a series of competitive experiments. In detail, **1** reacted preferentially with Se-Cys, **2** with Cys, and **3** with His, whereas **4** and **5** undergo redox reactions and oxidize Cys to cystine. Redox reactions were easily followed by mass spectrometry as long as the Au^{III} species was reduced to Au^{I} or by monitoring liberated chelating ligands. Compound **1** did not form adducts with the model proteins ub and cyt, but **2** and **3** were able to do so to an equal extent while retaining their C,N ligands. Compounds **4** and **5** formed higher order adducts with these proteins, but the gold center was found only in the +1 oxidation state in this case. The molecular reactivity patterns and binding preferences correlated with the inhibition of TrxR1, i.e., Se-Cys interaction leads to potent TrxR1 inhibitors and in some cases to a high antiproliferative activity. The binding preferences imply that the families of coordination and organometallic Au^{III} anticancer agents follow different modes of action. It is worth mentioning that the released ligand must also be considered when discussing the cytotoxic effects of these metal compounds. Adducts between the Au^{III} compounds and nucleotides were detected, although this occurred to different extents and with varying specificities for certain nucleotides.

Thus, although the structural complexity of the possible target biomolecules is a key player in the reactivity of

metallo drugs and further studies are warranted to fully define it, mass spectrometry was successfully applied to characterize molecular reactivities of gold drug candidates and to relate them to their biological effects. Importantly, this experimental setup can potentially be used for any metallo drug under conditions where forming a coordination bond is part of its mechanism of action.

■ ASSOCIATED CONTENT

■ Supporting Information

The Supporting Information is available free of charge on the ACS Publications website at DOI: [10.1021/acs.inorgchem.5b03000](https://doi.org/10.1021/acs.inorgchem.5b03000).

Materials, instrumentation, and experimental sections for MS and enzyme inhibition studies, as well as additional ESI-IT and ESI-TOF MS data and IC₅₀ assessment of 1–4 against TrxR1 and the A2780 cell line (PDF)

■ AUTHOR INFORMATION

Corresponding Authors

*(S.M.M.) E-mail: samuel.meier@univie.ac.at.

*(A.C.) E-mail: CasiniA@cardiff.ac.uk.

Notes

The authors declare no competing financial interest.

■ ACKNOWLEDGMENTS

A.C. thanks the University of Groningen for funding (Rosalind Franklin Fellowship). S.M.M. would like to thank Filip Groznica, Rebecca Maerz, and Markus Paunger for performing some of the ESI-IT MS measurements. The authors are grateful to EU COST Action CM1105 for fruitful discussions and opportunities to collaborate and to the University of Vienna for access to the Mass Spectrometry Core Facilities at the Faculty of Chemistry.

■ REFERENCES

- (1) Mjos, K. D.; Orvig, C. *Chem. Rev.* **2014**, *114*, 4540–4563.
- (2) Schmitt, F.; Freudenreich, J.; Barry, N. P.; Juillerat-Jeanneret, L.; Suss-Fink, G.; Therrien, B. *J. Am. Chem. Soc.* **2012**, *134*, 754–757.
- (3) Barragan, F.; Lopez-Senin, P.; Salassa, L.; Betanzos-Lara, S.; Habtemariam, A.; Moreno, V.; Sadler, P. J.; Marchan, V. *J. Am. Chem. Soc.* **2011**, *133*, 14098–14108.
- (4) Chen, H.; MacDonald, R. C.; Li, S.; Krett, N. L.; Rosen, S. T.; O'Halloran, T. V. *J. Am. Chem. Soc.* **2006**, *128*, 13348–13349.
- (5) Adhireksan, Z.; Davey, G. E.; Campomanes, P.; Groessl, M.; Clavel, C. M.; Yu, H.; Nazarov, A. A.; Yeo, C. H.; Ang, W. H.; Droge, P.; Rothlisberger, U.; Dyson, P. J.; Davey, C. A. *Nat. Commun.* **2014**, *5*, 3462.
- (6) Nobili, S.; Mini, E.; Landini, I.; Gabbiani, C.; Casini, A.; Messori, L. *Med. Res. Rev.* **2009**, *30*, 550–580.
- (7) Casini, A.; Messori, L. *Curr. Top. Med. Chem.* **2011**, *11*, 2647–2660.
- (8) Nagy, E. M.; Ronconi, L.; Nardon, C.; Fregona, D. *Mini-Rev. Med. Chem.* **2012**, *12*, 1216–1229.
- (9) Ali, M. R.; Panikkanvalappil, S. R.; El-Sayed, M. A. *J. Am. Chem. Soc.* **2014**, *136*, 4464–4467.
- (10) Meyer, A.; Bagowski, C. P.; Kokoschka, M.; Stefanopoulou, M.; Alborzina, H.; Can, S.; Vlecken, D. H.; Sheldrick, W. S.; Wolf, S.; Ott, I. *Angew. Chem., Int. Ed.* **2012**, *51*, 8895–8899.
- (11) Roder, C.; Thomson, M. J. *Drugs R&D* **2015**, *15*, 13–20.
- (12) Jatoi, A.; Radecki Breitkopf, C.; Foster, N. R.; Block, M. S.; Grudem, M.; Wahner Hendrickson, A.; Carlson, R. E.; Barrette, B.; Karlin, N.; Fields, A. P. *Oncology* **2015**, *88*, 208–213.
- (13) Bertrand, B.; Casini, A. *Dalton Trans.* **2014**, *43*, 4209–4219.

- (14) Liu, W. K.; Gust, R. *Chem. Soc. Rev.* **2013**, *42*, 755–773.
- (15) Oehninger, L.; Rubbiani, R.; Ott, I. *Dalton Trans.* **2013**, *42*, 3269–3284.
- (16) Cinellu, M. A.; Ott, I.; Casini, A. Gold Organometallics with Biological Properties. In *Bioorganometallic Chemistry*; Jaouen, G., Salmain, M., Eds.; Wiley-VCH: Weinheim, Germany, 2014; pp 117–140.
- (17) Casini, A.; Hartinger, C.; Gabbiani, C.; Mini, E.; Dyson, P. J.; Keppler, B. K.; Messori, L. *J. Inorg. Biochem.* **2008**, *102*, 564–575.
- (18) Glisic, B. D.; Rychlewska, U.; Djuran, M. I. *Dalton Trans.* **2012**, *41*, 6887–6901.
- (19) Gabbiani, C.; Casini, A.; Kelter, G.; Cocco, F.; Cinellu, M. A.; Fiebig, H. H.; Messori, L. *Metallomics* **2011**, *3*, 1318–1323.
- (20) Casini, A.; Cinellu, M. A.; Minghetti, G.; Gabbiani, C.; Coronello, M.; Mini, E.; Messori, L. *J. Med. Chem.* **2006**, *49*, 5524–5531.
- (21) Bindoli, A.; Rigobello, M. P.; Scutari, G.; Gabbiani, C.; Casini, A.; Messori, L. *Coord. Chem. Rev.* **2009**, *253*, 1692–1707.
- (22) Pratesi, A.; Gabbiani, C.; Ginanneschi, M.; Messori, L. *Chem. Commun.* **2010**, *46*, 7001–7003.
- (23) Pratesi, A.; Gabbiani, C.; Michelucci, E.; Ginanneschi, M.; Papini, A. M.; Rubbiani, R.; Ott, I.; Messori, L. *J. Inorg. Biochem.* **2014**, *136*, 161–169.
- (24) Schuh, E.; Pfluger, C.; Citta, A.; Folda, A.; Rigobello, M. P.; Bindoli, A.; Casini, A.; Mohr, F. *J. Med. Chem.* **2012**, *55*, 5518–5528.
- (25) Marcon, G.; Carotti, S.; Coronello, M.; Messori, L.; Mini, E.; Orioli, P.; Mazzei, T.; Cinellu, M. A.; Minghetti, G. *J. Med. Chem.* **2002**, *45*, 1672–1677.
- (26) Cocco, F.; Cinellu, M. A.; Minghetti, G.; Zucca, A.; Stoccoro, S.; Maiore, L.; Manassero, M. *Organometallics* **2010**, *29*, 1064–1066.
- (27) Cinellu, M. A.; Zucca, A.; Stoccoro, S.; Minghetti, G.; Manassero, M.; Sansoni, M. *J. Chem. Soc., Dalton Trans.* **1995**, 2865–2872.
- (28) Coronello, M.; Marcon, G.; Carotti, S.; Caciagli, B.; Mini, E.; Mazzei, T.; Orioli, P.; Messori, L. *Oncol. Res.* **2000**, *12*, 361–370.
- (29) Hollis, L. S.; Lippard, S. J. *J. Am. Chem. Soc.* **1983**, *105*, 4293–4299.
- (30) Meier, S. M.; Babak, M. V.; Keppler, B. K.; Hartinger, C. G. *ChemMedChem* **2014**, *9*, 1351–1355.
- (31) Peleg-Shulman, T.; Najajreh, Y.; Gibson, D. *J. Inorg. Biochem.* **2002**, *91*, 306–311.
- (32) Casini, A.; Gabbiani, C.; Mastrobuoni, G.; Messori, L.; Moneti, G.; Pieraccini, G. *ChemMedChem* **2006**, *1*, 413–417.
- (33) Casini, A.; Mastrobuoni, G.; Ang, W. H.; Gabbiani, C.; Pieraccini, G.; Moneti, G.; Dyson, P. J.; Messori, L. *ChemMedChem* **2007**, *2*, 631–635.
- (34) Gabbiani, C.; Casini, A.; Mastrobuoni, G.; Kirshenbaum, N.; Moshel, O.; Pieraccini, G.; Moneti, G.; Messori, L.; Gibson, D. *JBIC, J. Biol. Inorg. Chem.* **2008**, *13*, 755–764.
- (35) Meier, S. M.; Tsybin, Y. O.; Dyson, P. J.; Keppler, B. K.; Hartinger, C. G. *Anal. Bioanal. Chem.* **2012**, *402*, 2655–2662.
- (36) Peleg-Shulman, T.; Gibson, D. *J. Am. Chem. Soc.* **2001**, *123*, 3171–3172.
- (37) Estrella, V.; Chen, T.; Lloyd, M.; Wojtkowiak, J.; Cornnell, H. H.; Ibrahim-Hashim, A.; Bailey, K.; Balagurunathan, Y.; Rothberg, J. M.; Sloane, B. F.; Johnson, J.; Gatenby, R. A.; Gillies, R. J. *Cancer Res.* **2013**, *73*, 1524–1535.
- (38) Hartinger, C. G.; Groessl, M.; Meier, S. M.; Casini, A.; Dyson, P. J. *J. Chem. Soc. Rev.* **2013**, *42*, 6186–6199.
- (39) Gabbiani, C.; Massai, L.; Scaletti, F.; Michelucci, E.; Maiore, L.; Cinellu, M. A.; Messori, L. *JBIC, J. Biol. Inorg. Chem.* **2012**, *17*, 1293–1302.
- (40) Sanna, G.; Pilo, M.; Spano, N.; Minghetti, G.; Cinellu, M. A.; Zucca, A.; Seeber, R. *J. Organomet. Chem.* **2001**, *622*, 47–53.
- (41) Hartinger, C. G.; Ang, W. H.; Casini, A.; Messori, L.; Keppler, B. K.; Dyson, P. J. *J. Anal. At. Spectrom.* **2007**, *22*, 960–967.
- (42) Meier, S. M.; Novak, M. S.; Kandioller, W.; Jakupec, M. A.; Roller, A.; Keppler, B. K.; Hartinger, C. G. *Dalton Trans.* **2014**, *43*, 9851–9855.

- (43) Casini, A.; Mastrobuoni, G.; Temperini, C.; Gabbiani, C.; Francese, S.; Moneti, G.; Supuran, C. T.; Scozzafava, A.; Messori, L. *Chem. Commun.* **2007**, 156–158.
- (44) Gabbiani, C.; Casini, A.; Mastrobuoni, G.; Kirshenbaum, N.; Moshel, O.; Pieraccini, G.; Moneti, G.; Messori, L.; Gibson, D. *JBIC, J. Biol. Inorg. Chem.* **2008**, *13*, 755–764.
- (45) Casini, A.; Gabbiani, C.; Michelucci, E.; Pieraccini, G.; Moneti, G.; Dyson, P. J.; Messori, L. *JBIC, J. Biol. Inorg. Chem.* **2009**, *14*, 761–770.
- (46) Messori, L.; Cinellu, M. A.; Merlino, A. *ACS Med. Chem. Lett.* **2014**, *5*, 1110–1113.
- (47) Mendes, F.; Groessel, M.; Nazarov, A. A.; Tsybin, Y. O.; Sava, G.; Santos, I.; Dyson, P. J.; Casini, A. *J. Med. Chem.* **2011**, *54*, 2196–2206.
- (48) Laskay, U. A.; Garino, C.; Tsybin, Y. O.; Salassa, L.; Casini, A. *Chem. Commun.* **2015**, *51*, 1612–1615.
- (49) Beck, J. L.; Colgrave, M. L.; Ralph, S. F.; Sheil, M. M. *Mass Spectrom. Rev.* **2001**, *20*, 61–87.
- (50) Egger, A. E.; Hartinger, C. G.; Ben Hamidane, H.; Tsybin, Y. O.; Keppler, B. K.; Dyson, P. J. *Inorg. Chem.* **2008**, *47*, 10626–10633.
- (51) Talib, J.; Green, C.; Davis, K. J.; Urathamakul, T.; Beck, J. L.; Aldrich-Wright, J. R.; Ralph, S. F. *Dalton Trans.* **2008**, 1018–10126.
- (52) Talib, J.; Beck, J. L.; Urathamakul, T.; Nguyen, C. D.; Aldrich-Wright, J. R.; Mackay, J. P.; Ralph, S. F. *Chem. Commun.* **2009**, 5546–5548.
- (53) Rubbiani, R.; Zehnder, T. N.; Mari, C.; Blacque, O.; Venkatesan, K.; Gasser, G. *ChemMedChem* **2014**, *9*, 2781–2790.